A chlorophyll-retrieval algorithm for satellite imagery (Medium Resolution Imaging Spectrometer) of inland and coastal waters

HERMAN J. GONS*, MACHTELD RIJKEBOER[1,3] AND KEVIN G. RUDDICK[2]

NETHERLANDS INSTITUTE OF ECOLOGY, (NIOO-KNAW) CENTRE FOR LIMNOLOGY, RIJKSSTRAATWEG 6, NIEUWERSLUIS, PO BOX 1299, 3600 BG MAARSSEN, [1]INSTITUTE FOR ENVIRONMENTAL STUDIES, FREE UNIVERSITY, DE BOELELAAN 1115, 1081 HV AMSTERDAM, THE NETHERLANDS AND [2]MANAGEMENT UNIT OF THE MATHEMATICAL MODELS OF THE NORTH SEA, 100 GULLEDELLE, B-1200 BRUSSELS, BELGIUM

[3]PRESENT ADDRESS: NETHERLANDS INSTITUTE OF ECOLOGY, (NIOO-KNAW)CENTRE FOR LIMNOLOGY, RIJKSSTRAATWEG 6, NIEUWERSLUIS, PO BOX 1299, 3600 BG MAARSSEN, THE NETHERLANDS

*CORRESPONDING AUTHOR: gons@cl.nioo.knaw.nl.

A chlorophyll (Chl) a retrieval algorithm, originally developed for spectral subsurface irradiance reflectance determined from above-water shipboard measurements, was adapted for use with satellite imagery to be acquired by the MERIS (Medium Resolution Imaging Spectrometer) instrument. This MERIS algorithm was calibrated for Chl a concentrations in the range 3–185 mg m^{-3} using spectral reflectance calculated from shipboard measurements on the IJssel Lagoon (The Netherlands). Next, the algorithm was validated for various inland and coastal waters covering this concentration range. Despite the lower spectral resolution of MERIS as compared to the shipboard spectro-radiometer, the standard error of estimate is expected to be similar, i.e. ~9 mg m^{-3} of Chl a in mesotrophic and eutrophic lakes, rivers, estuaries and coastal waters.

INTRODUCTION

The Coastal Zone Colour Scanner (CZCS) aboard the Nimbus-7 satellite (1978–1986) has greatly increased our knowledge of the distribution of chlorophyll (Chl) *a* in the oceans and thereby of global primary production (Antoine *et al.*, 1995; Longhurst *et al.*, 1995; Behrenfeld and Falkowski, 1997). Successors of CZCS are the Sea-viewing Wide Field-of-view Sensor (SeaWiFS), in orbit since September 1997, and the Medium Resolution Imaging Spectrometer (MERIS) of the recent European environmental remote sensing satellite ENVISAT-1. The mission of MERIS includes quantifying distributions of phytoplankton in the open oceans and coastal waters, as well as of vegetation on the land surface (Rast *et al.*, 1999). Whereas CZCS incorporated five channels for the visible and near-infrared (NIR) ranges, for MERIS up to 15 wavebands can be selected. Compared to SeaWiFS, which lacks a channel for the red/NIR edge, MERIS appears to offer a better band suite for retrieval of Chl *a* in turbid waters. As detailed below, three of these bands

are similar to those used in an algorithm for shipboard optical teledetection of Chl *a* (Gons, 1999). The spatial resolution of 300 m at nadir allows the mapping of numerous lakes and reservoirs, a feature not foreseen in the original mission objectives (Rast *et al.*, 1999), as well as coastal seas.

A change in the concentration of Chl *a* causes a shift in the blue to green ratio of upwelling light in Case 1 waters, where the optical properties mainly depend on phytoplankton (Morel and Prieur, 1977; Prieur and Sathyendranath, 1981). However, this colour ratio cannot be used for the detection of Chl *a* in Case 2 waters, i.e. with strongly blue-light-absorbing dissolved organic matter (DOM) or detritus particles. For eutrophic lakes and rivers, the retrieval of Chl *a* is improved when a NIR to red ratio of spectral reflectance is used (Dekker *et al.*, 1991; Mittenzwey *et al.*, 1992). Further improvement is achieved by incorporating backscattering as computed from the NIR band of the irradiance reflectance at null depth [$R(0,\lambda)$, where λ denotes wavelength]. A semi-empirical relationship between the Chl *a* concentration

and $R(0,\lambda)$ determined for 672, 704 and 776 nm proved to hold for various lakes as well as for estuarine and coastal waters (Gons, 1999; Gons *et al.*, 2000).

The MERIS setting includes bands centred at 665, 705 and 775 nm with full-width half-maximum (FWHM) bandwidths of 10, 10 and 15 nm, respectively. The principal difference with the previous bands is the shorter wavelength near the red Chl *a* absorption peak. This 665 nm band has not been primarily selected to detect Chl *a* absorption, but to provide a baseline for fluorescence line height at 681 nm (Gower *et al.*, 1999). The present work addresses the potential retrieval of Chl *a* in turbid coastal and inland waters from reflectance at these MERIS bands. Reflectance spectra from shipboard above-water measurements served to emulate MERIS data, assuming perfect correction for atmospheric conditions.

METHOD

Previous work demonstrated that the concentration of Chl *a* can be estimated from the reflectance ratio R for λ = 704 and 672 nm, i.e. for the NIR reflectance peak in eutrophic water and the red absorption peak of Chl *a*, respectively, the absorption coefficients of water $a_w(\lambda)$ for these wavelengths, and the backscattering coefficient b_b (assumed to be wavelength independent) derived from the reflectance at λ = 776 nm (Gons, 1999):

$$[\text{Chl } a] = \{\text{R}(a_w(704) + b_b) - a_w(672) - b_b{}^p\} / a^*(672) \quad (1)$$

where the values of $a_w(672)$ and $a_w(704)$ are 0.415 and 0.630 m^{-1}, respectively (Buiteveld *et al.*, 1994), $a^*(672)$ is a mean Chl *a*-specific absorption coefficient at λ = 672 nm and p is an empirical constant close to unity.

The retrieval of Chl *a* was tested on $R(0,\lambda)$ deduced from above-water measurements made using a model

PR-650 SpectraColorimeter from Photo Research (Chatsworth, CA, USA) over the 380–780 nm range at 4 nm increments with 8 nm FWHM bandwidth (Gons, 1999). The reflectance values for 664, 704 and 776 nm calculated from the shipboard spectroradiometry were used to emulate $R(0,\lambda)$ for the relevant MERIS bands. The MERIS algorithm as referred to below is obtained following replacement in the original equation (1) of $R(0,\lambda)$ and $a_w(\lambda)$ for λ = 672 nm by the values for 664 nm:

$$[\text{Chl } a] = \{\text{R}_M(a_w(704) + b_b) - a_w(664) - b_b{}^p\} / a^*(664) \quad (2)$$

where R_M is the reflectance ratio for λ = 704 and 664 nm, and $a_w(664) = 0.402$ m^{-1}.

The MERIS algorithm was calibrated using data collected on the IJssel Lagoon (The Netherlands) in 1993–1996. Validation was performed using data on the IJssel Lagoon in 1997 and 1999, other Dutch inland waters and the Chinese Lake Tai Hu, the Scheldt Estuary (Belgium/The Netherlands) and Hudson/Raritan Estuary (New York/New Jersey), and the North Sea off the Belgian coast (Table I). Except for the IJssel Lagoon validation data, the reflectance spectra and physical and chemical conditions are presented in Gons (1999) and Gons *et al.* (Gons *et al.*, 2000). All concentrations of Chl *a* were determined after extraction in ethanol and correction for phaeopigment by acidification (Nusch, 1980).

RESULTS

The observations that had served the calibration of equation (1) (Gons, 1999) were used here to calibrate equation (2) for MERIS application. The model fit gave $p = 1.063 \pm 0.005$ and $a^*(664) = 0.0146 \pm 0.0002$ m^2 (mg of Chl a)$^{-1}$ (Figure 1; $n = 114$; $r^2 = 0.96$). Whereas the value of p remained the same, the coefficient $a^*(664)$ was significantly lower than $a^*(672) = 0.0176 \pm 0.0002$ in the

Table I: Calibration and validation of the prediction of concentrations of Chl a corrected for phaeopigment (Chl a) from spectral subsurface irradiance reflectance according to equation (2) (see text)

	n	Range	SE
IJssel Lagoon (calibration)	114	3–185	8.3
IJssel Lagoon (validation)	30	3–181	9.5
Other freshwater bodies	31	2–119	10.1
Estuarine and coastal waters	30	1–93	8.2
All validation data	91	1–181	9.2

n is the number of observations; range refers to Chl *a* concentrations (mg m^{-3}) in near-surface water samples; SE is the standard error of the estimate of Chl *a* concentration (mg m^{-3}).
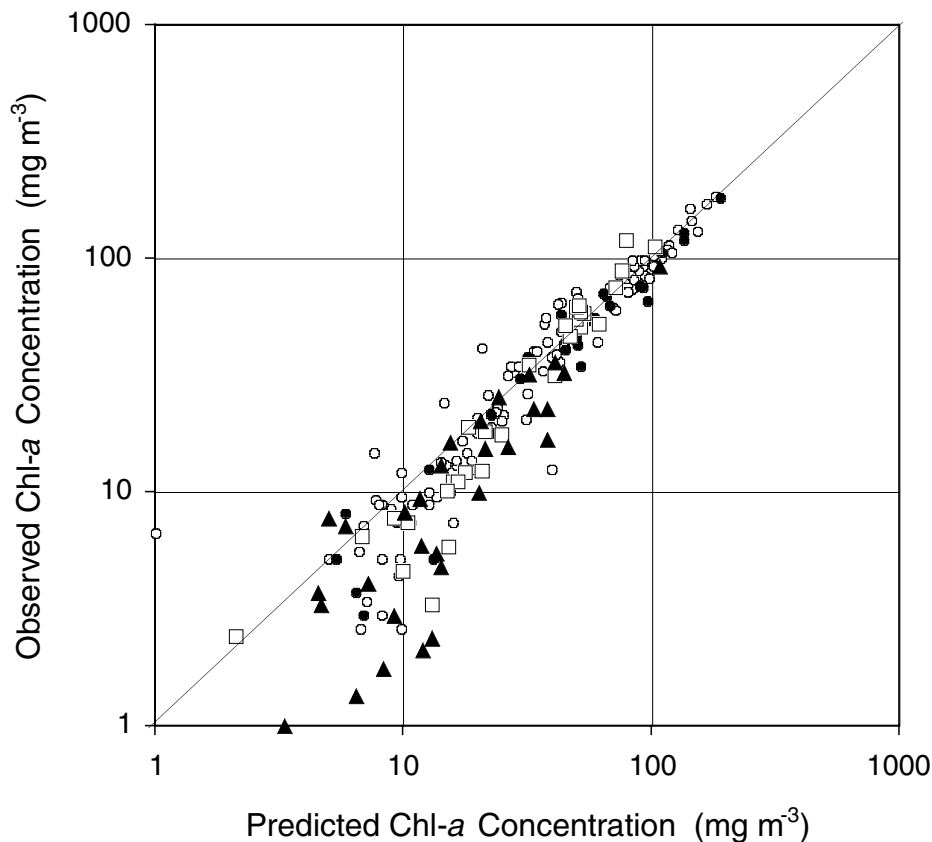
Fig. 1. Concentrations of Chl *a* corrected for phaeopigment (Chl *a*) in near-surface samples versus the values computed from subsurface spectral irradiance reflectance [equation (2); see text] for IJssel Lagoon (open circles, calibration data from 1993–1996; solid circles, observations made in 1997 and 1999), other inland waters (open squares), and estuarine and coastal waters (solid triangles).

original calibration. The departure from the pigment's red absorption maximum near 675 nm explains this lowered a^* value. Also, for uncorrected Chl *a* (Chl *a*-u = Chl *a* + phaeopigment/1.7), the exponent $p = 1.056$ remained the same, whilst $a^*(664) = 0.0127 \pm 0.0001$ was significantly lower than $a^*(672) = 0.0152 \pm 0.0002$ m^2 (mg of Chl *a*-u)$^{-1}$ in the original calibration.

The sensitivity of results to the different sensor bandwidth and slight shifts in wavelength of the other two bands was tested by simulating a lower resolution. The fit was found to be equally good when applying the averaged values of $R(0,\lambda)$ and $a_w(\lambda)$ for the PR-650 bands centred at 664 and 668 nm, 704 and 708 nm, and 772 and 776 nm. For both Chl *a* and Chl *a*-u, the value of p did not change. The values of a^* were 0.0162 and 0.0140 m^2 (mg of Chl *a*)$^{-1}$, respectively, and therefore between those for the 664 and 672 nm bands.

The potential of the MERIS instrument for Chl *a* detection in mesotrophic and eutrophic Case 2 waters for $p = 1.06$ and $a^*(664) = 0.0146$ m^2 (mg of Chl *a*)$^{-1}$ was

tested for later observations on the IJssel Lagoon, other freshwater bodies, and estuarine and coastal waters (see Method). The data were collected in widely different weather, and except for cases of floating layers of cyanobacteria and visible benthic vegetation, no observations were excluded for this work. The plots for validation and calibration of the MERIS algorithm compared very well (Figure 1). Neither this plot nor the standard of the estimate (SE) (Table I) for these groups of water bodies indicated a need for the development of regional algorithms.

DISCUSSION

By the use of the 664 nm instead of the 672 nm waveband, the MERIS algorithm might be less accurate than the original because the shorter wavelength is off the red absorption peak of Chl *a*. The error implicit in equations (1) and (2) by assumed negligible absorption other than by Chl *a* and water is enlarged, because of increased relative

importance of detritus particles and DOM at the shorter wavelength. Analyses of inland waters showed that detritus may absorb red light as strongly as water (Rijkeboer *et al.*, 1998). High concentrations of phaeopigment and humic substances could significantly increase the ratio R. The effect of such an increase on the prediction of Chl *a* [equations (1) and (2)] depends on both the pigment concentration and the backscattering. Sensitivity analysis showed that non-phytoplankton absorption may explain the tendency to overestimate Chl *a* for low concentrations (Figure 1), which did not show clearly in the previous work (Gons, 1999; Gons *et al.*, 2000).

Regarding the widely different phytoplankton encountered in the various water bodies, significant spread may have been due to variability in the value of a^* (Bricaud *et al.*, 1995). Other sources of data scatter were incomplete mixing, rapidly changing cloud, and water surface roughness, including prominent Langmuir streaks. Nevertheless, the validation provided satisfactory SE for the total data ($n = 91$) as well as for the separate groups of water bodies (Table I). Over the whole Chl *a* range, the calibration for MERIS gave somewhat lower SE than for the original algorithm.

True validation of this MERIS application can, of course, not be achieved until sufficient ground truth for the sensor in orbit. Theory indicates that the data can be accurately corrected for aerosols and water vapour. With three channels in the NIR range available for atmospheric correction, the sensor is optimized for observation of turbid waters (Moore *et al.*, 1999; Ruddick *et al.*, 2000). Different viewing of the PR-650 and MERIS instruments may cause significant discrepancies in the observation of water-leaving radiance, and thereby in the Chl *a* prediction. The view direction of MERIS can deviate markedly from the 90° azimuth and 42° nadir angles adopted for PR-650 operation. The use here of a reflectance ratio will minimize bidirectional effects, which are unlikely to vary much over the spectral range considered and will thus approximately cancel in the ratio.

More important than the view direction might be the fact that the diameter of MERIS pixels will be three orders of magnitude greater than for the PR-650 instrument. Contrary to stochastic variation in shipboard measurements, a satellite sensor may collect a stable signal, because the effects of waves and foam are averaged out over the area in view. Although stable, this signal may also be distorted by several factors. Provided viewing geometry is optimal and wind speeds are <5 m s^{-1}, the influence of sun glint will be small, and water-surface reflected sky light can be adequately subtracted from the water-leaving radiance (Mobley, 1999). Strong winds complicate this correction, especially for shallow waters exhibiting extensive foam from Langmuir streaks. The

Chl *a* retrieval may still be only slightly affected, because these perturbations change reflectance magnitude rather than spectral shape (Gons, 1999; Gons *et al.*, 2000).

The algorithm described here appears to offer a simple and robust alternative to the neural network approach, which will be used to provide the standard MERIS Chl *a* products in Case 2 waters (Schiller and Doerffer, 1999). The present study has demonstrated that this algorithm can be used to retrieve moderate to high concentrations of Chl *a* in very different water bodies without region-specific calibration. The MERIS sensor may indeed be used to survey distributions of phytoplankton in many Case 2 waters, and accelerate the understanding of physical and human impacts on ecosystem functioning on regional scales.

REFERENCES

Antoine, D., André, J.-M. and Morel, A. (1995) Oceanic primary production. 2. Estimation at global scale from satellite (Coastal Zone Color Scanner) chlorophyll. *Global Biogeochem. Cycles*, **10**, 57–69.

Behrenfeld, M. J. and Falkowski, P. G. (1997) Photosynthetic rates derived from satellite-based chlorophyll concentration. *Limnol. Oceanogr.*, **42**, 1–20.

Bricaud, A., Babin, M., Morel, A. and Claustre, H. (1995) Variability in the chlorophyll-specific absorption coefficients of natural phytoplankton: analysis and parameterization. *J. Geophys. Res.*, **100**, 13121–13332.

Buiteveld, H., Hakvoort, J. H. M. and Donze, M. (1994) The optical properties of pure water. *Ocean Opt. XII Proc. Soc. Photoopt. Inst. Eng.*, **2258**, 174–183.

Dekker, A. G., Malthus, T. J. and Seyhan, E. (1991) Quantitative modeling of inland water quality for high-resolution MSS systems. *IEEE Trans. Geosci. Remote Sens.*, **29**, 89–95.

Gons, H. J. (1999) Optical teledetection of chlorophyll *a* in turbid inland waters. *Environ. Sci. Technol.*, **33**, 1127–1132.

Gons, H. J., Rijkeboer, M., Bagheri, S. and Ruddick, K. G. (2000) Optical teledetection of chlorophyll *a* in estuarine and coastal waters. *Environ. Sci. Technol.*, **34**, 5189–5192.

Gower, J. F. R., Doerffer, R. and Borstad, G. A. (1999) Interpretation of the 685nm peak in water-leaving radiance spectra in terms of fluorescence, absorption and scattering, and its observation by MERIS. *Int. J. Remote Sens.*, **20**, 1771–1787.

Longhurst, A., Sathyendranath, S., Platt, T. and Caverhill, C. (1995) An estimate of global primary production in the ocean from satellite radiometer data. *J. Plankton Res.*, **17**, 1245–1271.

Mittenzwey, K.-H., Ullrich, S., Gitelson, A. A. and Kondratiev, K. Y.

(1992) Determination of chlorophyll *a* of inland waters on the basis of spectral reflectance. *Limnol. Oceanogr.*, **37**, 147–149.

Mobley, C. D. (1999) Estimation of the remote-sensing reflectance from above-surface measurements. *Appl. Opt.*, **38**, 7442–7455.

Moore, G. F., Aiken, J. and Lavender, S. J. (1999) The atmospheric correction of water colour and the quantitative retrieval of suspended particulate matter in Case II waters: application to MERIS. *Int. J. Remote Sens.*, **20**, 1713–1734.

Morel, A. and Prieur, L. (1977) Analysis of variations in ocean color. *Limnol. Oceanogr.*, **22**, 709–722.

Nusch, E. A. (1980) Comparison of different methods for chlorophyll and phaeopigment determination. *Arch. Hydrobiol. Beih. Ergebn. Limnol.*, **14**, 14–36.

Prieur, L. and Sathyendranath, S. (1981) An optical classification of coastal and oceanic waters based on the specific spectral absorption curves of phytoplankton pigments, dissolved organic matter, and other particulate materials. *Limnol. Oceanogr.*, **26**, 671–689.

Rast, M., Bezy, J. L. and Bruzzi, S. (1999) The ESA Medium Resolution Imaging Spectrometer MERIS—a review of the instrument and its mission. *Int. J. Remote Sens.*, **20**, 1681–1702.

Rijkeboer, M., Dekker, A. G. and Gons, H. J. (1998) Subsurface irradiance reflectance spectra of inland waters differing in morphometry and hydrology. *Aquat. Ecol.*, **31**, 313–323.

Ruddick, K. G., Ovidio, F. and Rijkeboer, M. (2000) Atmospheric correction of SeaWiFS imagery for turbid coastal and inland waters. *Appl. Opt.*, **39**, 897–912.

Schiller, H. and Doerffer, R. (1999) Neural network for emulation of an inverse model—operational derivation of Case II water properties from MERIS data. *Int. J. Remote Sens.*, **20**, 1735–1746.